ChemComm

Cite this: *Chem. Commun.*, 2011, **47**, 11504–11506

www.rsc.org/chemcomm

COMMUNICATION

A core-extended naphthalene diimide as a p-channel semiconductor†

Sabin-Lucian Suraru,[a] Ute Zschieschang,[b] Hagen Klauk*[b] and Frank Würthner*[a]

Received 18th August 2011, Accepted 12th September 2011
DOI: 10.1039/c1cc15144d

A novel naphthalene diimide with a fully conjugated, extended π-core was synthesized in a one-pot, two-step reaction. This organic semiconductor exhibits ambipolar transport properties with a large hole mobility of 0.56 cm^2 V^{-1} s^{-1} and a current *on/off* ratio of 10^6 in bottom-gate, top-contact thin-film transistors prepared by vacuum deposition.

Organic thin-film transistors (TFTs) have currently been the subject of intensive research activity due to their promising attributes for the manufacturing of low-cost, large-area and flexible electronic devices.[1] π-Conjugated polycyclic aromatic compounds are preferably used as semiconductor materials for small-molecule TFTs.[2] In particular, acenes[3] and heteroacenes[4] are efficient hole-transporting (p-type) semiconductors, whereas rylene diimides, especially perylene and naphthalene derivatives, are so far the most successful air-stable electron-transporting (n-type) materials.[5]

Naphthalene diimides (NDIs) are a versatile class of chromophores[6] owing to the convenient tunability of their optical and electrochemical properties by functionalization of the parent NDI core at the 2, 3, 6, 7 positions. In this regard, the introduction of electron-donating groups is a powerful tool to reduce the optical band gap of NDIs,[7] while the incorporation of electron-withdrawing groups at the core reduces the LUMO energy. The latter is a common approach in the design of organic n-type semiconductors.[8,9]

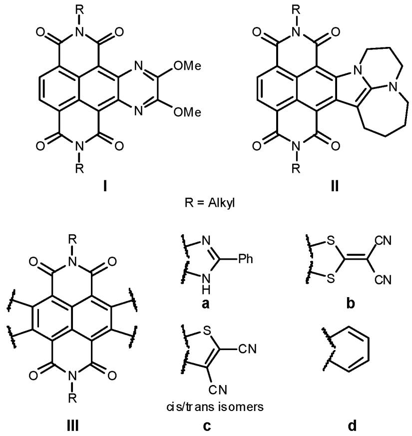

Chart 1 Core-extended NDIs reported so far in the literature.[12–16]

The expansion of the π-system along the long axis (N–N) of the parent NDI was synthetically realized many decades ago by derivatization of the imide groups into perinone vat dyes and pigments,[10] and in recent years by expansion of the carbocyclic scaffold beyond well-known perylene diimides up to hexarylene diimides.[11] In contrast, the lateral expansion of the NDI core has been demonstrated only recently. Examples that comprise the annulation of five- and six-membered heterocyclic rings either on one side of the NDI core (compounds **I**[12] and **II**[13] in Chart 1) or on both sides (compounds **IIIa**,[14] **IIIb**,**c**)[15] have been reported. Most interestingly, Zhu and coworkers have shown that the core-expanded NDIs **IIIb**,**c** with annulated sulfur-containing heterocycles bearing terminal electron-withdrawing groups exhibit n-type transport with electron mobilities similar to other NDIs.[9,15] Very recently, a tetracene diimide **IIId** has been reported that also exhibits n-type transport.[16] However, to the best of our knowledge, no core-extended NDIs showing p-type (hole) transport have been reported to date.

We expected that lateral expansion on both sides of the NDI core by fusion with highly electron-rich carbazole rings would lead to a p-type semiconducting axis orthogonal to the N–N axis responsible for n-type transport, as schematically depicted in Fig. 1a. For the realization of this concept, we have designed and synthesized the core-carbazole-annulated NDI **1** bearing diisopropylphenyl groups at the imide positions (Fig. 1b). These bulky imide substituents with branched alkyl chains have been chosen, on one hand, to achieve good solubility of the NDI and, on the other hand, to prevent molecular packing along the N–N axis, and hence to promote p-type transport by means of stacking of the π-core along the orthogonal electron-rich axis. Here we report that the newly designed NDI **1** indeed exhibits highly efficient p-channel transport, which is unprecedented for NDI-based semiconductors.

The core-expanded naphthalene diimide **1**, which is formally a carbazolo[2,3-*b*]carbazole-6,7 : 13,14-tetracarboxylic acid diimide, was synthesized by a one-pot, two-step reaction of the regioisomerically pure 2,6-dibromo NDI **2**[17] with 2-bromoaniline in the presence of potassium carbonate as a base and palladium(II) acetate as a catalyst (for the detailed

---

[a] *Universität Würzburg, Institut für Organische Chemie and Röntgen Research Center for Complex Material Systems, Am Hubland, 97074 Würzburg, Germany.
E-mail: wuerthner@chemie.uni-wuerzburg.de;
Fax: +49 (0)931 31 84756; Tel: +49 (0)931 31 85340*
[b] *Max Planck Institute for Solid State Research, Heisenbergstr. 1, 70569 Stuttgart, Germany. E-mail: H.Klauk@fkf.mpg.de;
Fax: +49 (0)711 689 1472; Tel: +49 (0)711 689 1401*

† Electronic supplementary information (ESI) available: Synthetic details, 1D and 2D NMR spectra, HRMS, cyclic voltammogram, and AFM image of **1**. See DOI: 10.1039/c1cc15144d

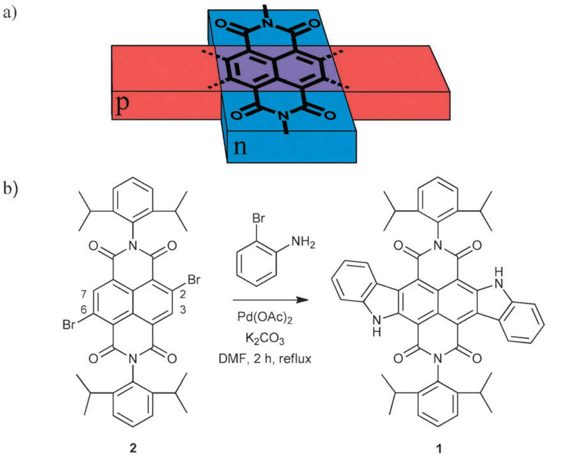

Fig. 1 (a) Schematic representation of the concept for π-conjugated systems with direction-dependent p- or n-type semiconducting characteristics. (b) Synthesis of laterally core-expanded NDI **1**.

synthetic procedure see ESI†). In this two-step reaction, the nucleophilic substitution of the bromine atoms at the NDI core with the amino group of 2-bromoaniline,[18] and an *in situ* palladium-catalyzed intramolecular arylation[19] of the NDI core with the bromoaryl moiety lead to the formation of carbazole-annulated NDI derivative **1**. Column chromatographical purification of the crude product and subsequent recycling GPC afforded highly pure NDI **1** in 12% isolated yield. This new NDI derivative is fully characterized by 1D and 2D NMR spectroscopy, high-resolution mass spectrometry, and elemental analysis (for the characterization data see ESI†, Fig. S1–S6).

The optical properties of NDI **1** were investigated by UV-vis absorption and emission spectroscopy in dichloromethane (Fig. 2). Compound **1** forms a green solution in dichloromethane resulting from two absorption bands with maxima at 622 nm and 491 nm. Moreover, it shows a weak red fluorescence with a maximum at 641 nm. Hence, from the intersection of absorption and emission spectra an optical band gap of 1.96 eV was determined. The redox properties of NDI **1** were characterized by cyclic voltammetry against the potential of the ferrocenium/ferrocene redox couple in dichloromethane (Fig. S7, see ESI†). Two reversible reductions with half-wave potentials at −1.49 and −1.07 V, respectively, and an irreversible oxidation with a peak potential at 1.11 V were observed. From these CV data the energy levels of the frontier molecular orbitals (FMOs) of NDI **1** were obtained by using 4.80 eV as the ionization potential for ferrocene.[20] Thus, for the lowest unoccupied molecular orbital (LUMO) an energy level of −3.73 eV and for the highest occupied molecular orbital (HOMO) an energy of −5.91 eV (from the peak potential) were estimated. The LUMO and HOMO energy levels of NDI **1** were calculated by the DFT method as well, revealing values of −3.40 and −5.76 eV, respectively, which are in good accordance with the experimental values obtained from cyclic voltammetry data. The frontier orbitals of **1** calculated by the DFT method reveal that in the LUMO the electron density is mainly localized on the parent NDI core, while the HOMO is delocalized in the orthogonal direction over the whole expanded π-system (Fig. 3). This implies that n-type transport in this laterally core-extended NDI should be possible if the dyes pack with displacements only along the N–N axis (longitudinal displacements), since the electron transport in organic semiconductors occurs in the LUMO, while p-type transport (which involves the HOMO) should be supported if the dyes pack only with displacements perpendicular to the N–N axis (transversal displacements). Thus, the electronic features of the frontier orbitals of NDI **1** comply with our concept proposed in Fig. 1a. Owing to the presence of bulky imide substituents in NDI **1**, however, a packing with π–π-contacts can only be expected with significant transversal displacements which is expected to suppress the electron transport and favour the hole transport capability of this particular NDI derivative.

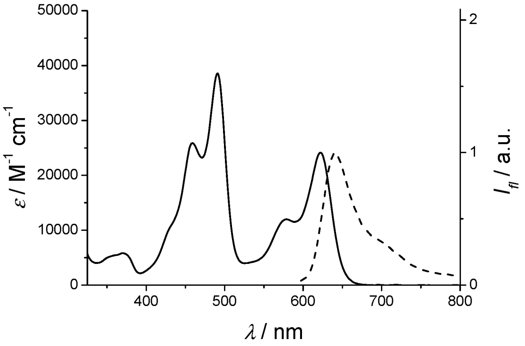

Fig. 2 Absorption (solid line) and emission (λ_{ex} = 446 nm, dashed line) spectra of **1** in dichloromethane measured at a concentration of 10^{-5} and $<10^{-6}$ M, respectively.

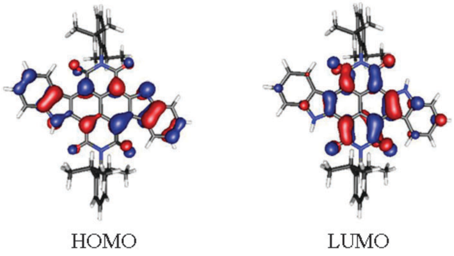

Fig. 3 HOMO (left) and LUMO (right) of **1** according to DFT (B3-LYP) calculations.

To explore the viability of our concept, we have investigated the semiconducting properties of NDI **1** in TFTs prepared by vacuum deposition. A bottom-gate, top-contact TFT with a 108 nm thick SiO_2/AlO_x gate dielectric functionalized with a fluoroalkyl phosphonic acid self-assembled monolayer (SAM) was fabricated, where the organic compound was deposited at a substrate temperature of 100 °C. Fig. 4 shows the output and transfer characteristics of this TFT measured in ambient air. This TFT exhibits p-type behaviour with a field-effect mobility of 0.56 cm^2 V^{-1} s^{-1} and an *on*/*off* current ratio of 10^6.

The morphology of the thin film was investigated by AFM, which is a useful tool to determine the degree of crystallinity of thin-film surfaces. Fig. S8 (see ESI†) depicts an AFM image of **1** in the measured device, revealing well-ordered crystalline domains formed during the evaporation process, which favour high-mobility charge-carrier transport.

The electron mobility in the TFTs with the 108 nm thick SiO_2/AlO_x gate dielectric is vanishingly small, regardless of whether the gate dielectric is functionalized with a fluoroalkyl or an alkyl phosphonic acid. We have also fabricated TFTs with a thinner gate dielectric (3.6 nm thick AlO_x + fluoroalkyl

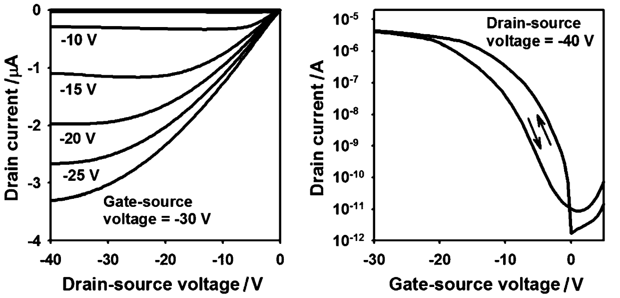

Fig. 4 Output and transfer characteristics of NDI **1** in a bottom-gate, top-contact TFT with a 108 nm thick SiO_2/AlO_x gate dielectric functionalized with a fluoroalkyl phosphonic acid SAM in p-channel operation.

or alkyl phosphonic acid SAM)[21] that show more balanced mobilities of 0.03 $cm^2\ V^{-1}\ s^{-1}$ for holes and 0.02 $cm^2\ V^{-1}\ s^{-1}$ for electrons (see Fig. S9 and Table S1, in ESI†). These results reveal that NDI **1** is indeed an ambipolar semiconductor with the dominant type of charge carrier being dependent on the TFT architecture.

The observed excellent p-type transport behaviour of NDI **1**, which is so far unprecedented for NDIs, can be related to its structural features that influence the molecular packing. The bulky diisopropylphenyl substituents in the imide positions of NDI **1** may suppress the intermolecular LUMO interactions, due to the perpendicular orientation of these substituents with respect to the core plane. On the other hand, the stacking of the extended π-core along the orthogonal axis is expected to be favoured, allowing an efficient HOMO overlap and thus large p-channel mobilities.[22]

In conclusion, we have designed a novel NDI derivative **1** with a fully π-conjugated core consisting of six annulated rings. The flat, extended conjugated core of this NDI enables charge-carrier transport in thin films, showing p- and n-type behaviour. The large hole mobility observed in TFTs of NDI **1** under p-channel operation can be explained in terms of its structural properties that favour intermolecular HOMO overlap by stacking of the extended π-core. Further studies to substantiate our novel concept presented here by studying a larger series of derivatives of NDI **1** bearing substituents that lead to other packing arrangements and their crystallographic analysis are the focus of our upcoming research work.

Financial support from the German Ministry of Education and Research (BMBF) for this work within the project POLYTOS (FKZ: 13N10205) in the Leading Edge Cluster "Forum Organic Electronics" is gratefully acknowledged.

Notes and references

1 *Organic Field-Effect Transistors*, ed. Z. Bao and J. Locklin, Taylor and Francis, Boca Raton, USA, 2007; H. Klauk, *Chem. Soc. Rev.*, 2010, **39**, 2643; A. C. Arias, J. D. MacKenzie, I. McCulloch, J. Rivnay and A. Salleo, *Chem. Rev.*, 2010, **110**, 3.

2 A. Facchetti, *Mater. Today*, 2007, **10**, 28; W. Wu, Y. Liu and D. Zhu, *Chem. Soc. Rev.*, 2010, **39**, 1489.

3 J. E. Anthony, *Angew. Chem., Int. Ed.*, 2008, **47**, 452; M. L. Tang and Z. Bao, *Chem. Mater.*, 2011, **23**, 446.

4 K. Takimiya, H. Ebata, K. Sakamoto, T. Izawa, T. Otsubo and Y. Kunugi, *J. Am. Chem. Soc.*, 2006, **128**, 12604; M. L. Tang, A. D. Reichardt, T. Siegrist, S. C. B. Mannsfeld and Z. Bao, *Chem. Mater.*, 2008, **20**, 4669; S. Subramanian, S. K. Park, S. R. Parkin, V. Podzorov, T. N. Jackson and J. E. Anthony, *J. Am. Chem. Soc.*, 2008, **130**, 2706; P. Gao, D. Beckmann, H. N. Tsao, X. Feng, V. Enkelmann, M. Baumgarten, W. Pisula and K. Müllen, *Adv. Mater.*, 2009, **21**, 213.

5 Y. Wen and Y. Liu, *Adv. Mater.*, 2010, **22**, 1331; X. Zhan, A. Facchetti, S. Barlow, T. J. Marks, M. A. Ratner, M. R. Wasielewski and S. R. Marder, *Adv. Mater.*, 2011, **23**, 268; F. Würthner and M. Stolte, *Chem. Commun.*, 2011, **47**, 5109; B. J. Jung, N. J. Tremblay, M.-L. Yeh and H. E. Katz, *Chem. Mater.*, 2011, **23**, 568.

6 S. V. Bhosale, C. H. Jani and S. J. Langford, *Chem. Soc. Rev.*, 2008, **37**, 331; N. Sakai, J. Mareda, E. Vauthey and S. Matile, *Chem. Commun.*, 2010, **46**, 4225.

7 C. Röger and F. Würthner, *J. Org. Chem.*, 2007, **72**, 8070.

8 B. A. Jones, A. Facchetti, T. J. Marks and M. R. Wasielewski, *Chem. Mater.*, 2007, **19**, 2703; J. H. Oh, S.-L. Suraru, W.-Y. Lee, M. Könemann, H. W. Höffken, C. Röger, R. Schmidt, Y. Chung, W.-C. Chen, F. Würthner and Z. Bao, *Adv. Funct. Mater.*, 2010, **20**, 2148.

9 X. Gao, C.-A. Di, Y. Hu, X. Yang, H. Fan, F. Zhang, Y. Liu, H. Li and D. Zhu, *J. Am. Chem. Soc.*, 2010, **132**, 3697; Y. Zhao, C.-A. Di, X. Gao, Y. Hu, Y. Guo, L. Zhang, Y. Liu, J. Wang, W. Hu and D. Zhu, *Adv. Mater.*, 2011, **23**, 2448.

10 W. Herbst and K. Hunger, *Industrial Organic Pigments, Production, Properties, Applications*, Wiley-VCH, Weinheim, 1997.

11 Y. Avlasevich, C. Li and K. Müllen, *J. Mater. Chem.*, 2010, **20**, 3814.

12 F. Doria, M. di Antonio, M. Benotti, D. Verga and M. Freccero, *J. Org. Chem.*, 2009, **74**, 8616.

13 C. Zhou, Y. Li, Y. Zhao, J. Zhang, W. Yang and Y. Li, *Org. Lett.*, 2011, **13**, 292.

14 H. Langhals and S. Kinzel, *J. Org. Chem.*, 2010, **75**, 7781.

15 Y. Hu, X. Gao, C.-A. Di, X. Yang, F. Zhang, Y. Liu, H. Li and D. Zhu, *Chem. Mater.*, 2011, **23**, 1204.

16 S. Katsuta, K. Tanaka, Y. Maruya, S. Mori, S. Masuo, T. Okujima, H. Uno, K. Nakayama and H. Yamada, *Chem. Commun.*, 2011, **47**, 10112.

17 C. Thalacker, C. Röger and F. Würthner, *J. Org. Chem.*, 2006, **71**, 8098; S. Chopin, F. Chaignon, E. Blart and F. Odobel, *J. Mater. Chem.*, 2007, **17**, 4139; X. Lu, W. Zhu, Y. Xie, X. Li, Y. Gao, F. Li and H. Tian, *Chem.–Eur. J.*, 2010, **16**, 8355.

18 F. Würthner, S. Ahmed, C. Thalacker and T. Debaerdemaeker, *Chem.–Eur. J.*, 2002, **8**, 4742.

19 D. Alberico, M. E. Scott and M. Lautens, *Chem. Rev.*, 2007, **107**, 174; L. Ackermann, R. Vincente and A. R. Kapdi, *Angew. Chem., Int. Ed.*, 2009, **48**, 9792.

20 B. W. D'Andrade, S. Datta, S. R. Forrest, P. Djurovich, E. Polikarpov and M. E. Thompson, *Org. Electron.*, 2005, **6**, 11.

21 U. Zschieschang, F. Ante, M. Schlörholz, M. Schmidt, K. Kern and H. Klauk, *Adv. Mater.*, 2010, **22**, 4489.

22 Bulky substituents have been shown to be beneficial for the stacking behaviour of 6,13-disubstituted pentacenes, showing slip-stacking and thus enhanced intermolecular π-overlap: J. E. Anthony, J. S. Brooks, D. L. Eaton and S. R. Parkin, *J. Am. Chem. Soc.*, 2001, **123**, 9482; J. E. Anthony, D. L. Eaton and S. R. Parkin, *Org. Lett.*, 2002, **4**, 15.

Electronic supplementary information (ESI) for:

A core-extended naphthalene diimide as p-channel semiconductor

Sabin-Lucian Suraru,[a] Ute Zschieschang,[b] Hagen Klauk*,[b] and Frank Würthner*,[a]

[a] Universität Würzburg, Institut für Organische Chemie and Röntgen Research Center for Complex Material Systems, Am Hubland, 97074 Würzburg, Germany; Fax: +49 (0)931 31 84756; Tel: +49 (0)931 31 85340; E-mail: wuerthner@chemie.uni-wuerzburg.de
[b] Max Planck Institute for Solid State Research, Heisenbergstr. 1, 70569 Stuttgart, Germany; Fax: +49 (0)711 689 1472; Tel: +49 (0)711 689 1401; E-mail: H.Klauk@fkf.mpg.de

Table of contents

1. General methods

The starting compound *N*,*N*′-bis-(2′,6′-diisopropylphenyl)-2,6-dibromonaphthalene-1,4,5,8-tetracarboxylic acid diimide was prepared according to the literature.[1] All other reagents and solvents were obtained from commercial suppliers and purified and dried according to standard procedures.[2] Column chromatography was performed on silica gel (Merck Silica 60, particle size 0.040-0.063 mm). A preparative recycling GPC LC-9105, Japan Analytical Industry Co., Ltd. (JAI) with JAIGEL 2H+2.5H columns was used. Solvents for spectroscopic studies were of spectroscopic grade and used as received. ^{1}H and ^{13}C spectra were recorded in CD_2Cl_2 on a Bruker DMX 600 spectrometer. Residual undeuterated solvent was used as internal standard (5.32 ppm for ^{1}H, 53.80 ppm for ^{13}C). High-resolution ESI-TOF mass spectrometry was carried out on a microTOF focus instrument (Bruker Daltronik GmbH). UV-vis measurements were performed in CH_2Cl_2 (10^{-5} M) in a conventional quartz cell (light pass 10 mm) on a Perkin-Elmer Lambda 950 spectrometer. Fluorescence quantum yields were determined under dilute conditions in CH_2Cl_2 ($<10^{-6}$ M) versus *N,N'*-bis(2,6-diisopropylphenyl)-1,6,7,12-tetraphenoxyperylene-3,4:9,10-tetracarboxylic acid bisimide ($\Phi_f = 0.96$ in $CHCl_3$).[3] For cyclic voltammetry, a standard commercial electrochemical analyzer (EC epsilon; BAS Instruments, UK) with a three electrode single-compartment cell was used. Dichloromethane (HPLC grade) was dried over calcium hydride under argon and degassed before using. The supporting electrolyte tetrabutylammonium hexafluorophosphate (TBAHFP) was prepared according to the literature,[4] and recrystallized from ethanol/water. The measurements were carried out in dichloromethane at a concentration of about 10^{-4} M with ferrocene (Fc) as an internal standard for the calibration of the potential. Ag/AgCl reference electrode was used. A Pt disc and a Pt wire were used as working and auxiliary electrodes, respectively.

2. Experimental procedures, analytical and spectroscopic data

N,N′-Bis(2,6-diisopropylphenyl)-5*H*,12*H*-carbazolo[2,3-b]carbazol[6,7:13,14]-bis(tetracarboxylic acid diimide) 1

N,N′-Di-(2′,6′-diisopropylphenyl)-2,6-dibromonaphthalene-1,4,5,8-tetracarboxylic acid diimide **2** (60.0 mg, 80.6 µmol), 2-bromoaniline (38.8 mg, 0.226 mmol), $Pd(OAc)_2$ (5.4 mg, 0.024 mmol) and K_2CO_3 (22.3 mg, 0.161 mmol) were placed under argon and dry DMF (5 mL) was added. The mixture was refluxed in an oil-bath (175 °C) for 2 h. The solvent was removed under reduced pressure and the residue was purified by column chromatography (dichloromethane / pentane 1:1) and recycling-GPC affording **1** as a black solid (7.2 mg, 12%).

^{1}H NMR (600 MHz, CD_2Cl_2): 11.52 (s, 2H), 9.71 (d, $^3J = 7.3$ Hz, 2H), 7.74 – 7.71 (m, 2H), 7.70 – 7.67 (m, 2H), 7.62 (t, $^3J = 7.9$ Hz, 2H), 7.47 (d, $^3J = 7.9$ Hz, 2H), 7.40 – 7.36 (m, 2H), 2.92 (sept, $^3J = 6.9$ Hz, 4H), 1.20 (2x d, $^3J = 6.9$ Hz, 24H).

^{13}C NMR (151 MHz, CD_2Cl_2):166.0, 164.9, 146.6, 144.7, 142.8, 131.6, 131.4, 131.0, 130.5, 130.1, 124.7, 122.2, 121.6, 121.1, 120.0, 111.7, 105.07, 29.66, 24.14, 24.11.

HRMS (ESI, acetonitrile/$CHCl_3$ 1:1, pos.-mode): calcd for $C_{50}H_{45}N_4O_4$ 765.3435. Found 765.3433 $[M+H]^+$.

Elemental Anal. Calcd. for $C_{50}H_{44}N_4O_4$: C, 78.51; H, 5.80; N, 7.32; O, 8.37. Found: C, 78.75; H, 5.84; N, 7.39.

CV (CH_2Cl_2, 0.1 M TBAHFP, vs. Fc/Fc^+): $E_{1/2}^{red}$ $(X^-/X^{2-}) = -1.49$ V, $E_{1/2}^{red}$ $(X/X^-) = -1.07$ V, E_p^{ox} $(X/X^+) = 1.11$ V.

UV-vis (CH_2Cl_2): λ_{max} (ε) = 622 nm (ε = 24200), 491 nm (ε = 38600 L mol^{-1} cm^{-1}). Fluorescence (CH_2Cl_2, λ_{ex} = 446 nm): λ_{max} = 641 nm; Φ_{Fl} = 5%.

3. ^{1}H NMR, ^{13}C NMR spectra and ESI-HRMS

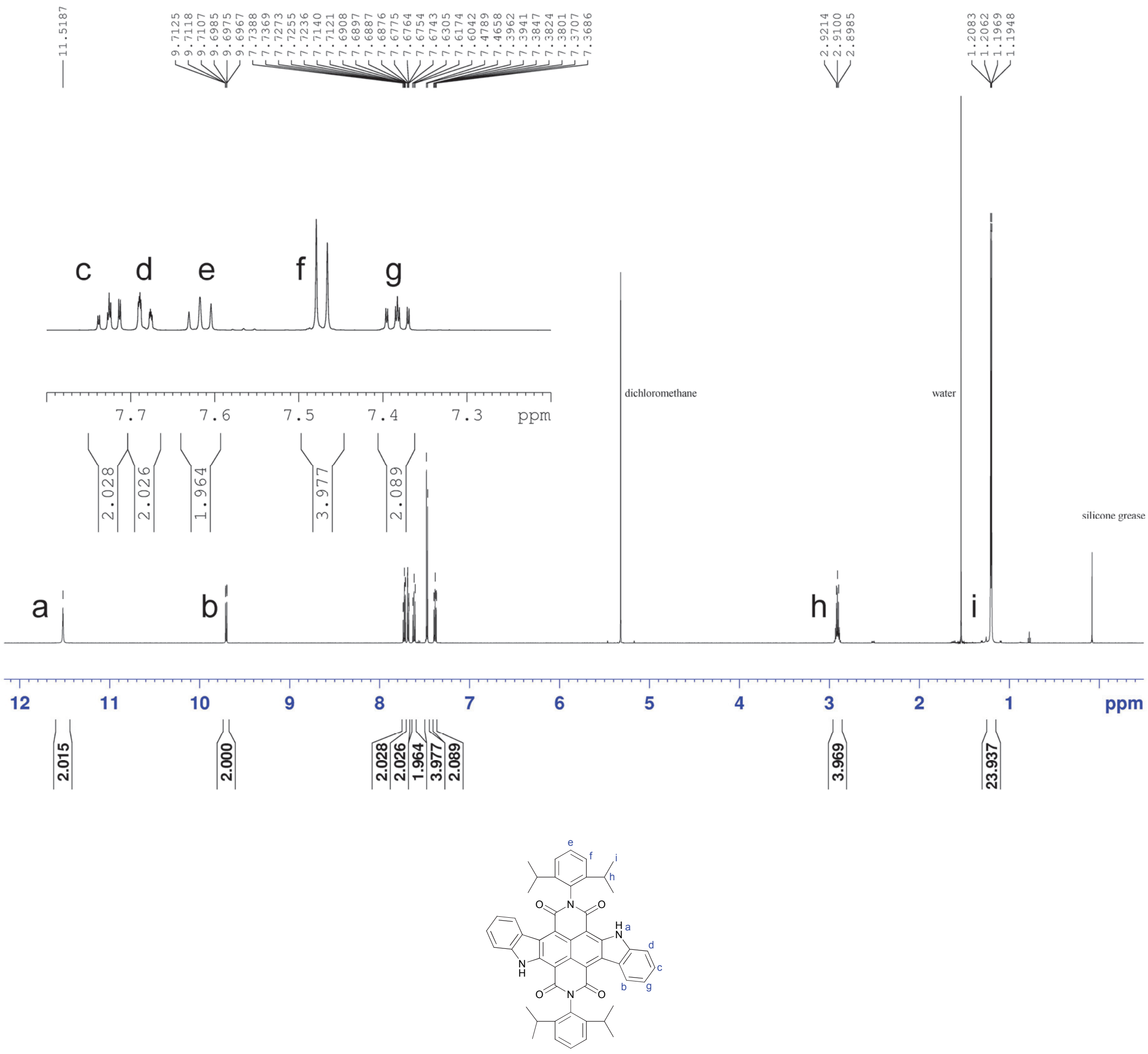

Fig. S1 ^{1}H NMR spectrum (600 MHz) of NDI **1** in CD_2Cl_2 and structural correlation of the signals.

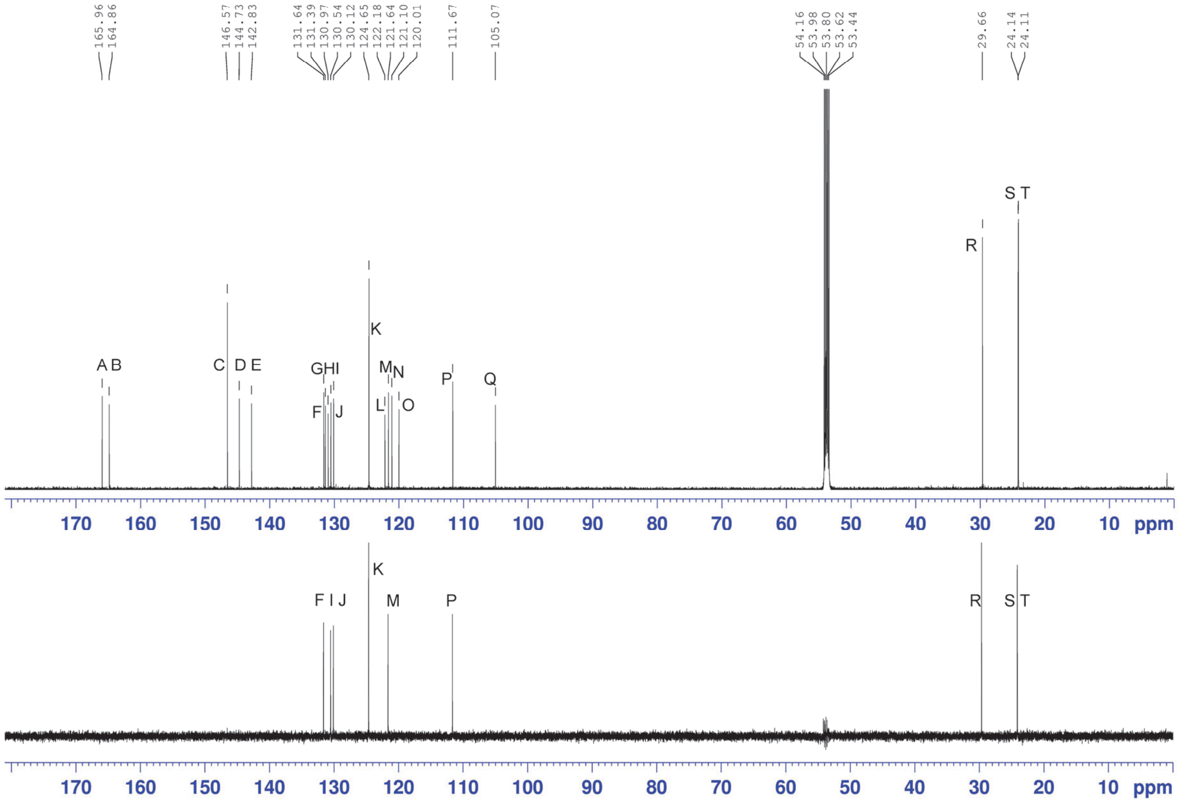

Fig. S2 ^{13}C NMR and DEPT-135 (151 MHz) spectra of NDI **1** in CD_2Cl_2.

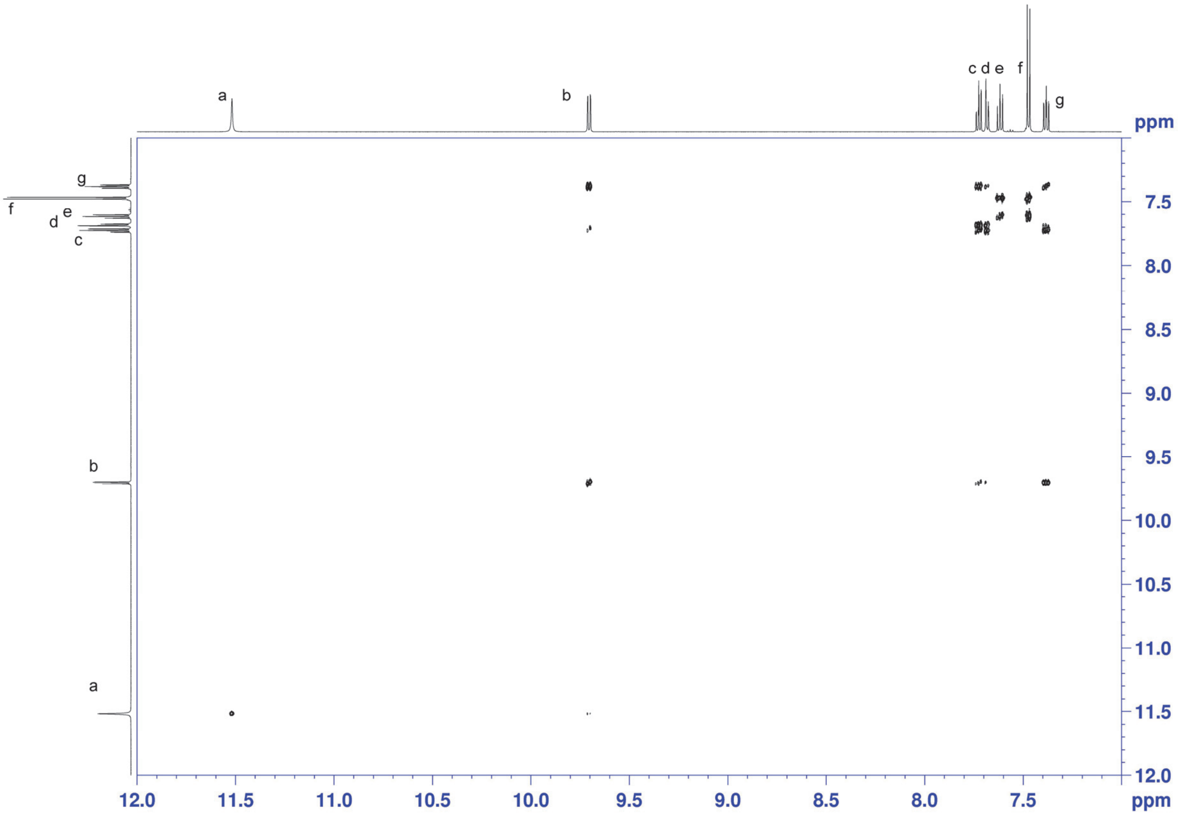

Fig. S3 COSY 45 spectrum of NDI **1** in CD_2Cl_2.

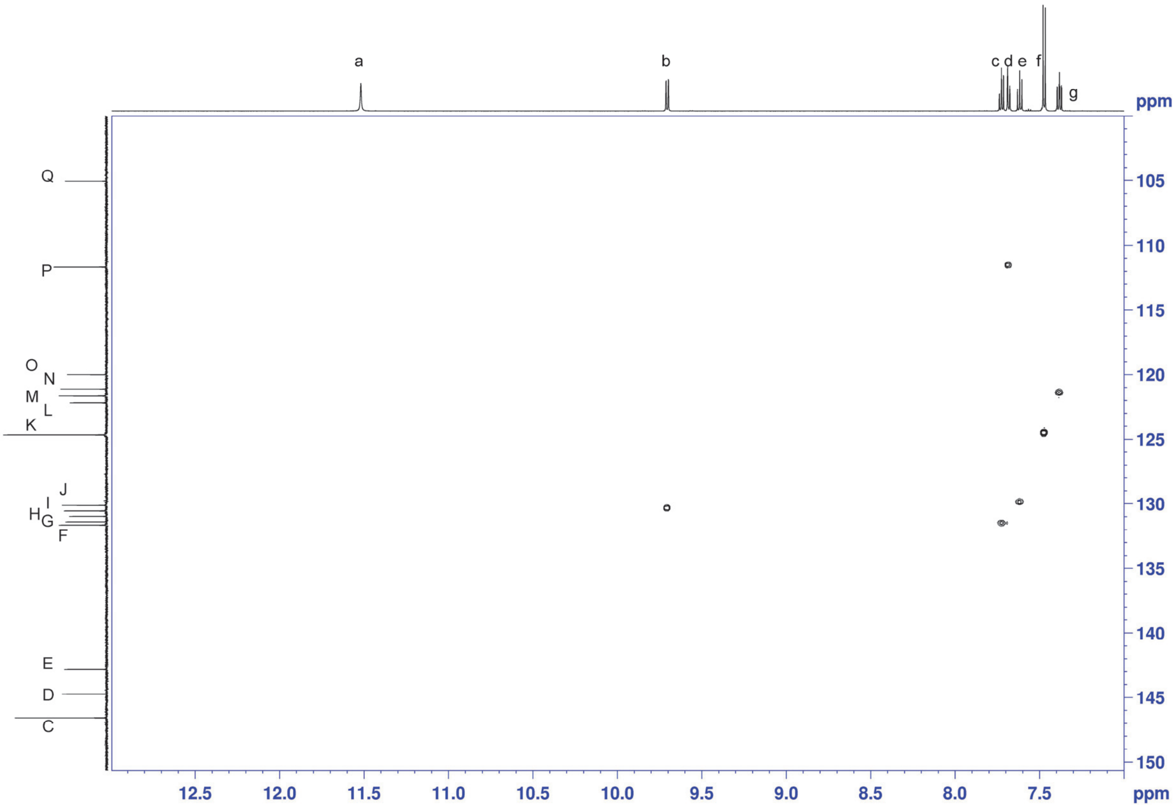

Fig. S4 HSQC spectrum of NDI **1** in CD_2Cl_2.

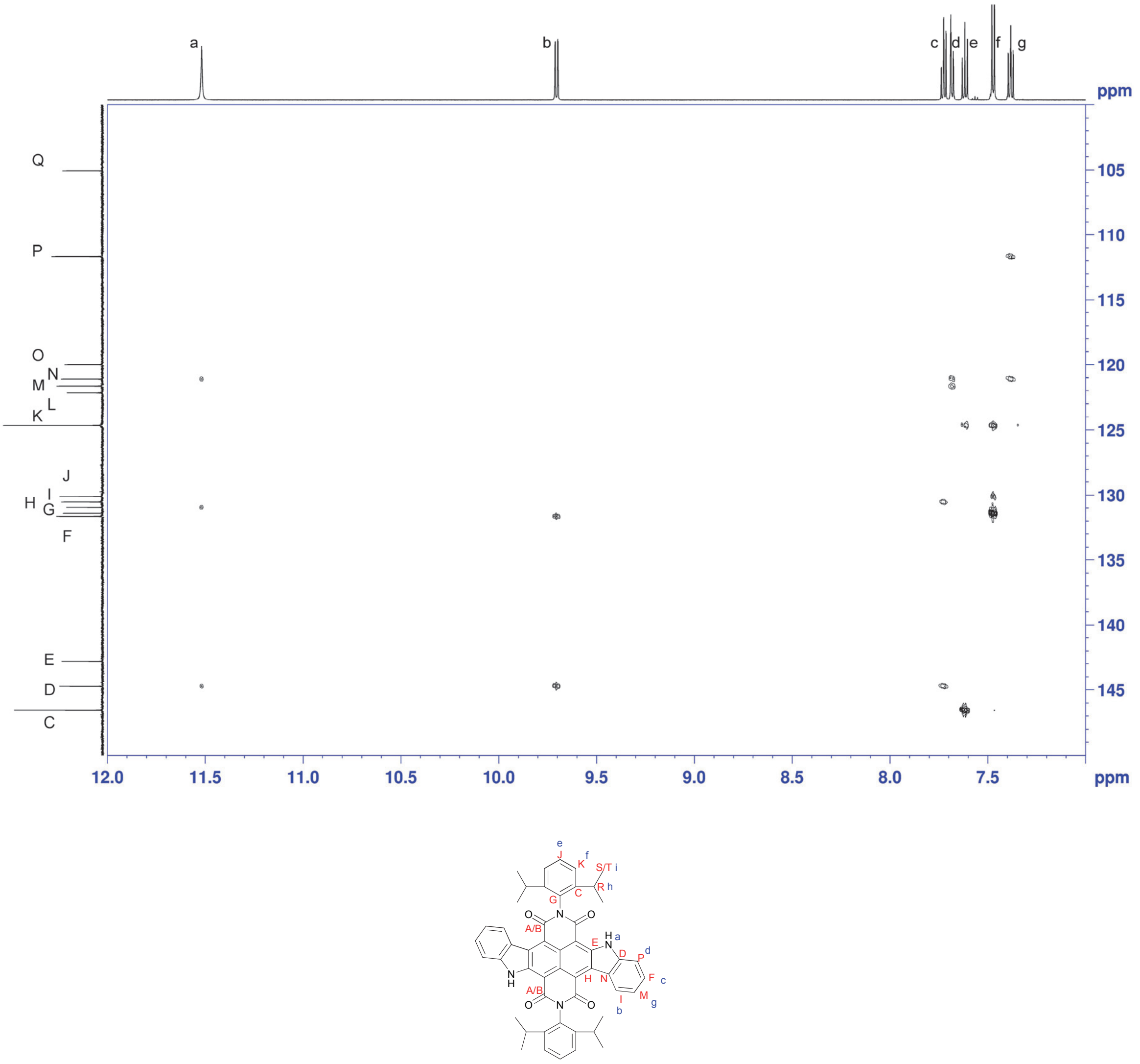

Fig. S5 HMBC spectrum of NDI **1** in CD_2Cl_2 and structural correlation of the signals.

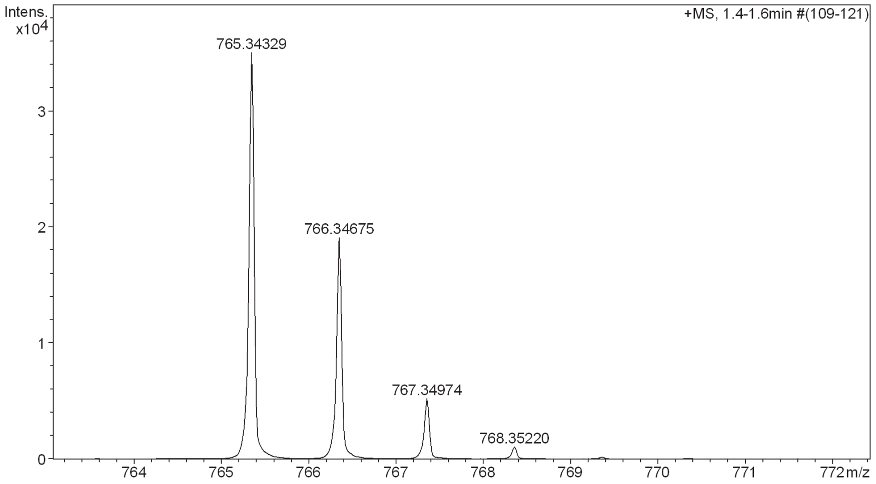

Fig. S6 High-resolution ESI-TOF mass spectrum of NDI **1** in acetonitrile/chloroform 1:1.

4. Cyclic voltammogram

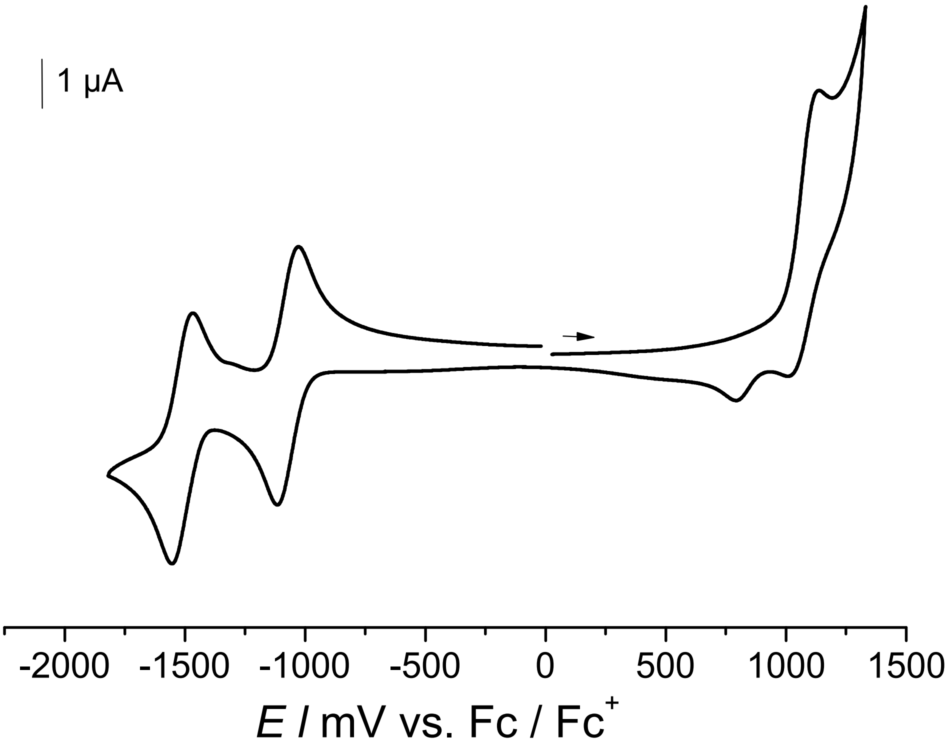

Fig. S7 Cyclic voltammogram of **1** in dichloromethane (10^{-4} M) using ferrocene as an internal standard at a of scan rate 100 mV s^{-1}; supporting electrolyte: tetrabutylammonium hexafluorophosphate (NBu_4PF_6, 0.1 M).

5. Theoretical investigations

NDI **1** was calculated with the DFT method in combination with the B3-LYP[5] functional. The calculations were performed with the TURBOMOLE program (version 5.10).[6] The TZVP[7] basis for C, N, O, and S atoms was combined with the TZV[6] basis for the H atom. This basis is designated as TZV(P) and was found to be an excellent compromise between accuracy and computational effort for systems of similar size.[8] NDI **1** was fully geometry-optimized, emanating from a structure computed on semi-empirical AM1 level.

6. Fabrication and characterization of organic TFTs and AFM

Organic TFTs were fabricated based on two different architectures: one with a thick SiO_2/AlO_x/SAM gate dielectric, the other with a thin AlO_x/SAM gate dielectric. In both cases, heavily doped silicon was used as the substrate. For the TFTs with the thick SiO_2/AlO_x/SAM gate dielectric, the silicon substrate was thermally oxidized to obtain a 100 nm thick layer of SiO_2, which was then covered with an 8 nm thick layer of AlO_x grown by atomic layer deposition (ALD). The $Si/SiO_2/AlO_x$ substrate was then immersed in a 2-propanol solution of 12,12,13,13,14,14,15,15,16,16,17,17,18,18,18-pentadecylfluoro-octadecylphosphonic acid (FC18-PA) or tetradecylphosphonic acid (HC14-PA) to allow a densely packed monolayer with a thickness of 2.1 nm (FC18-PA) or 1.7 nm (HC14-PA) to self-assemble on the AlO_x surface. In principle, phosphonic acid SAMs can also be obtained on SiO_2, but we have found that AlO_x is a more suitable surface for high-quality phosphonic acid SAMs. The total thickness of the SiO_2/AlO_x/SAM gate dielectric is about 110 nm.

For the TFTs with the thin AlO_x/SAM gate dielectric, a 20 nm thick aluminum gate electrode was first deposited onto the silicon substrate by thermal evaporation. The aluminum was then briefly exposed to an oxygen plasma to obtain 3.6 nm thick AlO_x, on the surface of which a self-assembled monolayer with a thickness of 2.1 nm (FC18-PA) or 1.7 nm (HC14-PA) was obtained from a 2-propanol solution. The total thickness of the AlO_x/SAM gate dielectric is 5.7 nm in the case of FC18-PA and 5.3 nm in case of HC14-PA.

A 30 nm thick layer of the organic semiconductor NDI **1** was then deposited onto the SAM by thermal sublimation in a vacuum evaporator at a substrate temperature of 100 °C. TFTs were completed by evaporating 30 nm thick gold source and drain contacts through a polyimide shadow mask, defining a channel length of 100 µm and a channel width of 200 µm. The current-voltage characteristics were measured using an Agilent 4156C Semiconductor Parameter Analyzer in ambient air.

The AFM images were processed with WSXM, a freeware scanning probe microscopy software.[9]

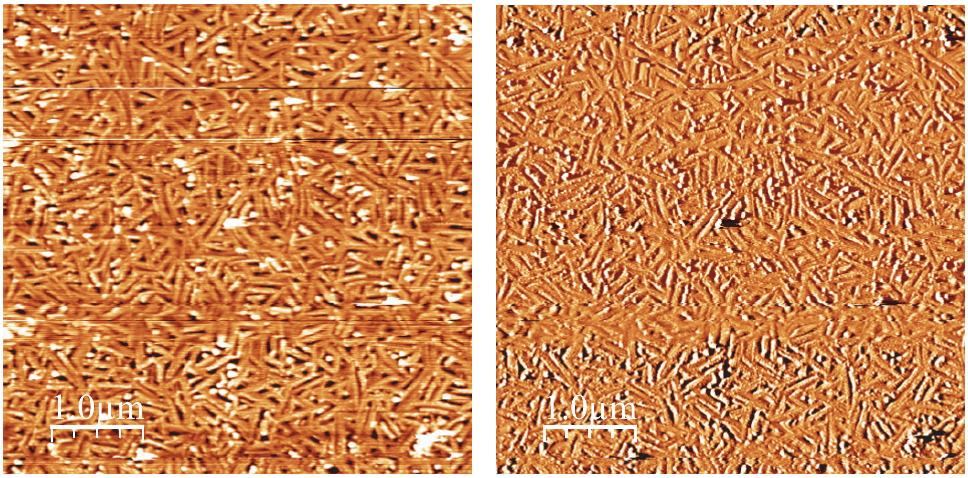

Fig. S8 AFM topography (left) and amplitude (right) images of vacuum deposited thin films of **1** onto SiO_2/AlO_x/SAM gate dielectric deposited at a substrate temperature of 100 °C.

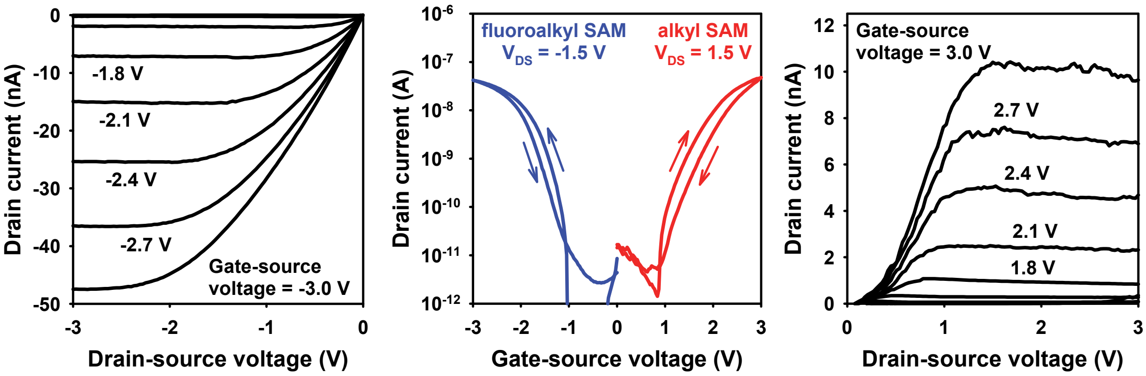

Fig. S9 Output and transfer characteristics of two TFTs based on the semiconductor NDI **1** with thin AlO_x/SAM gate dielectrics in which the SAM is composed either of a fluoroalkyl phosphonic acid (FC18-PA) or an alkyl phosphonic acid (HC14-PA).

Table S1 Field-effect mobilities measured for p-channel (holes) and n-channel operation (electrons) in TFTs based on NDI **1** using either thick SiO_2/AlO_x/SAM or thin AlO_x/SAM gate dielectrics.

gate dielectric	**hole mobility (cm^2/Vs)**	**electron mobility (cm^2/Vs)**
SiO_2 / AlO_x / FC18-PA SAM	0.56	$<10^{-5}$
SiO_2 / AlO_x / HC14-PA SAM	0.01	$\sim10^{-5}$
AlO_x / FC18-PA SAM	0.03	$<10^{-5}$
AlO_x / HC14-PA SAM	0.007	0.02

7. References

1 S. Chopin, F. Chaignon, E. Blart and F. Odobel, *J. Mater. Chem.*, 2007, **17**, 4139.

2 D. D. Perrin, W. L. Armarego, D. R. Perrin, *Purification of Laboratory Chemicals* –Pergamon Press Ltd.: Oxford, 1980, 2nd edn.

3 R. Gvishi, R. Reisfeld and Z. Burshtein, *Chem. Phys. Lett.* 1993, **213**, 338.

4 A. J. Fry, in *Laboratory Techniques in Electroanalytical Chemistry*, ed. Peter Kissinger and William R. Heineman, Marcel Dekker Ltd., New York; 1996, 2nd edn.

5 A. D. Becke, *Phys. Rev. A,* 1988, **38**, 3098; C. Lee, W. Yang and R. G. Parr; *Phys. Rev. B,* 1988, **37**, 785; A. D. Becke, *J. Chem. Phys.* 1993, **98**, 5648.

6 R. Ahlrichs, M. Bär, M. Häser, H. Horn and C. Köhmel, *Chem. Phys. Lett.,* 1989, **162**, 165; R. Ahlrichs and M. von Arnim, *Methods and Techniques in Computational Chemistry: METECC-95*; Clementi, E.; Corongiu, G., Eds.; Club Européen MOTECC, 1995.

7 A. Schäfer, C. Huber and R. Ahlrichs, *J. Chem. Phys.,* 1994, **100**, 5829.

8 R. F. Fink, J. Seibt, V. Engel, M. Renz, M. Kaupp, S. Lochbrunner, H.-M. Zhao, J. Pfister, F. Würthner and B. Engels, *J. Am. Chem. Soc.,* 2008, **130**, 12858.

9 I. Horcas, R. Fernandez, J. M. Gomez-Rodriguez, J. Colchero, J. Gomez-Herrero, A. M. Baro, *Rev. Sci. Instrum.,* 2007, **78**, 013705-1.